Ponticulin Is An Atypical Membrane Protein

Anne L. Hitt, Tze Hong Lu, and Elizabeth J. Luna

Worcester Foundation for Experimental Biology, Shrewsbury, Massachusetts 01545

Abstract. We have cloned and sequenced ponticulin, a 17,000-dalton integral membrane glycoprotein that binds F-actin and nucleates actin assembly. A single copy gene encodes a developmentally regulated message that is high during growth and early development, but drops precipitously during cell streaming at ~8 h of development. The deduced amino acid sequence predicts a protein with a cleaved NH_2-terminal signal sequence and a COOH-terminal glycosyl anchor. These predictions are supported by amino acid sequencing of mature ponticulin and metabolic labeling with glycosyl anchor components. Although no α-helical membrane-spanning domains are apparent, several hydrophobic and/or sided β-strands, each long enough to traverse the membrane, are predicted. Although its location on the primary sequence is unclear, an intracellular domain is indicated by the existence of a discontinuous epitope that is accessible to antibody in plasma membranes and permeabilized cells, but not in intact cells. Such a cytoplasmically oriented domain also is required for the demonstrated role of ponticulin in binding actin to the plasma membrane in vivo and in vitro (Hitt, A. L., J. H. Hartwig, and E. J. Luna. 1994. Ponticulin is the major high affinity link between the plasma membrane and the cortical actin network in *Dictyostelium*. *J. Cell Biol.* 126:1433–1444). Thus, ponticulin apparently represents a new category of integral membrane proteins that consists of proteins with both a glycosyl anchor and membrane-spanning peptide domain(s).

INTERACTIONS between the plasma membrane and the actin-based cytoskeleton are thought to be responsible for membrane stability and for its organization into specialized domains, e.g., for adhesion (18). Changes in cell shape and movement also are thought to be controlled by actin-membrane associations. Although most of these interactions apparently involve intermediary proteins (for reviews see references 6, 8, 31, 34, 47, 69), a small, but growing number of direct linkages between actin and membranes are known. For instance, both the EGF receptor (17) and the N-formyl peptide receptor (37) have been recently reported to bind directly to F-actin.

Ponticulin, a 17-kD glycoprotein first isolated from *Dictyostelium discoideum* plasma membranes (76), is another direct link between actin and the plasma membrane (49). A potential ponticulin analogue also has been observed in another amoeboid cell type, the human polymorphonuclear leukocyte (77).

Ponticulin accounts for as much as 96% of the in vitro actin-binding activity of *Dictyostelium* plasma membranes (76), as well as essentially all of the actin nucleation activity mediated by these membranes (59). An abundant membrane protein, ponticulin averages ~10^6 copies per cell with an estimated surface density of ~300 per μm^2 (11). Purified ponticulin binds directly and specifically to F-actin (10, 78), and, after reconstitution into vesicles with *Dictyostelium* lipid, promotes actin assembly (11). Ponticulin-associated actin nuclei have both ends free for monomer assembly (11, 59), consistent with a role for ponticulin in the previously observed lateral association of actin filaments with these membranes (25).

Although present throughout the plasma membrane, ponticulin appears to be preferentially localized in some actin-rich membrane structures (77). These structures include sites of cell–cell adhesion and arched regions of the plasma membrane suggestive of nascent pseudopods. Ponticulin also colocalizes with cortical F-actin (77) and cosediments with Triton-insoluble actin-containing cytoskeletons (11, 77). These observations suggest that ponticulin may function in vivo to attach and nucleate actin filaments at the cytoplasmic surface of the plasma membrane, a prediction borne out by analyses of cell lacking ponticulin (30).

The actin-binding site on ponticulin appears to be charged and discontinuous. Actin binding is inhibited by 2 M sodium chloride (76), indicating that the interaction with ponticulin is primarily electrostatic. Reduction of ponticulin with thiol reagents eliminates actin binding (10), suggesting that the actin-binding site is composed of non-contiguous residues in a conformation stabilized by disulfide bonds. Intact disulfide bonds also are required for recognition of ponticulin by a polyclonal antibody (R67 IgG)[1] called R67 IgG recognizing native ponticulin (77). Univalent fragments of R67 IgG

Address all correspondence to Dr. Anne L. Hitt, Worcester Foundation for Experimental Biology, 222 Maple Avenue, Shrewsbury, MA 01545. Telephone: (508) 842-8921; FAX: (508) 842-3915.

The current address of Dr. Tze Hong Lu is the Department of Medicine, University of Massachusetts Medical Center, 55 Lake Avenue North, Worcester, MA 01655.

1. *Abbreviations used in this paper*: PCR-RACE, polymerization chain reaction-mediated rapid amplification of cDNA ends; R67 IgG, rabbit IgG recognizing native ponticulin.

block actin binding to purified plasma membranes (77), suggesting that this antibody binds ponticulin at or near the actin-binding site.

We report in this manuscript the primary sequence of ponticulin and propose a model for the structure of this protein in the plasma membrane. Surprisingly, analysis of the deduced amino acid sequence predicts that ponticulin contains a cleaved NH_2-terminal signal sequence, four or six short hydrophobic β-strands, and a glycosyl anchor. We confirm the existence of a cytoplasmic domain and show that ponticulin is metabolically labeled with glycosyl anchor components. Thus, ponticulin apparently represents a new type of membrane protein, defined as integral membrane proteins possessing both a glycosyl anchor and transmembrane peptide domains.

Materials and Methods

Cell Culture

D. discoideum, strain AX3K, were grown at 21°C in shaking suspension (200 rpm) on HL-5 medium (12). After transformation with plasmids containing *Dictyostelium* DNA, *E. coli*, strain SURE® cells (Stratagene, La Jolla, CA), were grown at 30°C on media containing 25 μg/ml ampicillin. The lower temperature appeared to facilitate the stability of the *Dictyostelium* DNA inserts.

DNA Isolation and Southern Analysis

Dictyostelium genomic DNA was isolated as described (51). Plasmid DNA was isolated by the boiling mini-prep method (3) and further purified using USBioclean (United States Biochemical Corp., Cleveland, OH). Large scale preparation of plasmid DNA was by alkaline lysis and $CsCl_2$ gradient centrifugation (56). DNA (10 μg) was digested, electrophoretically separated, transferred to Duralon membrane (Stratagene), and cross-linked with UV radiation in a Stratalinker (Stratagene). The blot was prehybridized ≥30 min in hybridization buffer (7% SDS, 0.25 M sodium phosphate, pH 7.2, 10 mM EDTA, pH 7.2), and then probed overnight at 65°C with ^{32}P-labeled pT715A (see below). The blot was rinsed 2 × 5 min with hybridization buffer at 20°C, and then 3 × 15 min in 2 × SSC, 1% SDS at 65°C, and finally 3 × 15 min in 0.2 × SSC, 0.1% SDS at 65°C.

Library Construction

Because screens of several *Dictyostelium* cDNA libraries were unsuccessful, a size-selected *Dictyostelium* genomic library was constructed. DNA (100 μg) was cut with EcoRI and HindIII, and the restriction fragments sized by centrifugation through a 5–25% NaCl gradient in 10 mM Tris, 10 mM EDTA, pH 8.0 (56). DNA was collected as 0.3-ml fractions with a model 640 density gradient fractionator (Instrument Specialties Company, Lincoln, NE), diluted with TE (10 mM Tris, 1 mM EDTA, pH 8.0), and precipitated with ethanol.

The codon usage tables of Warrick and Spudich (73) were used to generate VK11, a "best-guess" oligonucleotide corresponding to the first 22 residues of the ponticulin NH_2 terminus (78). VK11 is 5'-CAATATACTTTATCAGTTTCAAATTCAGCTTCAGGTTCAAAATGTACTACTGCTGTTTCAGCTAAA-3'. ^{32}P-labeled VK11 was used to probe a Southern blot containing the fractionated *Dictyostelium* genomic DNA. The blot was hybridized at 55°C for 9 h in Wash A (4 × SET, 10 × Denhardt's solution, 0.1% SDS, 0.1% sodium pyrophosphate, 1% heparin) (72) and washed 2 × 5 min at room temperature with Wash A, 1 × 10 min at 55°C with Wash A, and 1 × 10 min at 55°C with Wash B (3 × SET, 0.1% SDS, 0.1% sodium pyrophosphate). DNA fragments from VK11-binding fractions were ligated into EcoRI/HindIII double-digested Bluescript® II KS(−) and used to transform SURE® cells (3). Duplicate colony lifts were screened at 55°C with VK11 as described above.

RNA Preparation and Northern Blot Analysis

After washing with 14.6 mM KH_2PO_4, 2.0 mM Na_2HPO_4, pH 6.0 (Sorensen's buffer), cells were either processed immediately (0 h cells) or were plated at ~10^8 cells per 10-cm Petri plates containing 1.5% bacto-agar (wt/vol) in Sorensen's buffer. Development was continued at room temperature (20–21°C) for 24 h. At 2-h intervals, developing cells were rinsed off the plates with 10 ml Sorensen's buffer, centrifuged 5 min at 300 *g*, and resuspended with a minimal volume of Sorensen's buffer into a thick slurry. Cells were lysed with 5% (wt/vol) SDS, 10 mM Tris-HCl, 10 mM EDTA, pH 8.0, 1 mg/ml proteinase K (Boehringer Mannheim Biologicals, Indianapolis, IN) for ≥4 h at 50°C. Sodium acetate (3 M, pH 7.0) was added to a final concentration of 0.3 M. RNA was extracted with phenol-chloroform (1:1), precipitated with isopropanol, resuspended in DEPC-treated water, and reextracted with acidic phenol-chloroform (51). RNA was separated on formaldehyde-agarose gels, vacuum blotted to Duralon (Stratagene), UV-cross-linked, and hybridized with ^{32}P-labeled pT715A, as described above.

Polymerization Chain Reaction–mediated Rapid Amplification of CDNA Ends

The 3'-end of the ponticulin-coding region was obtained using a modification of the polymerization chain reaction–mediated rapid amplification of cDNA ends (PCR-RACE) technique (21). First strand cDNA was synthesized from 5 μg of 0 h polyA$^+$-RNA. PolyA$^+$-RNA and 10 μM RACE hybrid primer (5'-GACTCGAGTCGACATCGA(T_{17})-3') in 5 μl DEPC-treated water were heated to 70°C for 10 min and quickly chilled on ice. Then, the following were added: 2 μl 0.1 M DTT, 4 μl 5 × buffer H-reverse transcriptase (Boehringer Mannheim), 1 μl 10 mM dNTP stock (Pharmacia LKB Biotechnology, Piscataway, NJ), 1 μl RNasin (Promega, Madison, WI), and 3.5 μl water. After heating to 37°C for 2 min, the reaction was started by the addition of 1 μl Moloney-Murine Reverse Transcriptase. After 1 h, the cDNA was heated to 90°C for 5 min, quickly chilled on ice, and either used immediately or stored at −70°C.

PCR reactions were performed as described in the protocol (Perkin Elmer-Cetus, Norwalk, CT). Briefly, 100-μl reactions contained 1 μl of cDNA, 0.1 μM RACE adaptor primer (5'-GACTCGAGTCGACATCG-3'), and 0.1 μM of 5'-CCGGAATTCGAAATTTATTAGCTTTAG-3', a primer containing an EcoRI cloning site and sequence corresponding to nt 14-31 of the ponticulin-coding region. The cycles were as follows: 1 × 2 min at 92°C; 40 × (1 min at 92°C, 1 min at 35°C, 30-s ramp, and 1.5 min at 72°C), and 1 × 10 min at 72°C. Polymerase was removed with 10 μl StrataClean™ resin (Stratagene). The DNA was cut with ClaI and EcoRI, extracted with phenol:chloroform (1:1), ethanol-precipitated, and ligated into Bluescript (56).

DNA Sequencing

Double-stranded exonuclease III deletion constructs were sequenced by the dideoxy chain termination method (57). pT715A is a ~500-bp genomic deletion fragment that includes the *ponA* TATA box. Both strands of the genomic coding region were sequenced as were seven clones generated by PCR-RACE. Comparisons with protein sequences in SWISS-PROT 28.0, PIR 39.0, and GenBank Release 83.0 (June 15, 1994) were performed at the National Center for Biotechnology Information (Bethesda, MD) using the BLAST network service (1, 7).

Antibodies

R67 IgG, also called anti-$NaIO_4$-PM IgG, is a rabbit polyclonal antibody raised against periodate-treated, NaOH-extracted *Dictyostelium* plasma membranes (76). After adsorption against glutaraldehyde-fixed log-phase cells, R67 IgG specifically recognizes all the 17-kD ponticulin isoforms (10, 76, 77). For all experiments described herein, R67 IgG was adsorbed 5–10 times with glutaraldehyde-fixed log-phase cells before use.

Anti-NaOH-PM IgG (anti-carbohydrate IgG) is a control antibody raised against NaOH-extracted *Dictyostelium* plasma membranes with intact cell surface carbohydrates (76). This antibody binds to a number of plasma membrane proteins with ~92% of the epitopes exposed on the cell surface. Most of this titer appears to be against highly immunogenic carbohydrate residues.

Metabolic Labeling and Immunoprecipitation

Log-phase AX3K cells were centrifuged, washed, and resuspended to ~10^7 cells/ml with Sorensen's buffer. Portions (5 ml) were incubated at 21°C with 1–2 mCi ^{3}H-labeled palmitic acid (New England Nuclear Dupont, Wilmington, DE) or with 0.5 mCi ^{3}H-labeled ethanolamine-HCl (Amersham Searle Corp., Arlington Heights, IL) for ~6 h with shaking (150 rpm). Free radiolabel was removed by pelleting and washing cells with Sorensen's buffer.

Crude membranes were prepared from the radiolabeled cells by filter lysis and sedimentation through a 10% (wt/vol) sucrose cushion (14). The pellet was resuspended, washed once with IgG buffer, frozen rapidly in a dry ice/ethanol bath, and stored at −80°C until use.

Ponticulin was immunoprecipitated with adsorbed R67 IgG from radiolabeled crude membranes (~20 μg) that had been solubilized with RIPA buffer (28, 76). Preimmune IgG from the same rabbit was used as a control. Immunoprecipitates were analyzed on 0.75-mm thick 10–20% polyacrylamide gradient gels (44). Gels were fixed, treated with EN^{3}HANCE (New England Nuclear Dupont) for 1 h, rinsed briefly with water, vacuum dried, and exposed to Kodak X-omat film with an intensifying screen at −80°C.

Glycosyl Anchor Enzyme Treatments

Plasma membranes (100 μg), purified from amoebae developed in suspension for 12 h (35, 36), were incubated for ≤6.5 h at 37°C with up to 1.75 U of *B. thuringiensis* PI-PLC (a generous gift from Dr. M. G. Low) in 100 mM Tris-HCl, pH 7.5. Parallel incubations were performed with as much as 5 U of human placental sphingomyelinase (Sigma Chem. Co., St. Louis, MO) in 0.1 M $MgCl_2$, 0.025% Triton X-100, 75 mM sodium acetate, pH 5.0.

Membrane Preparations

Purified plasma membranes were prepared from log-phase cells either by the Con A stabilization/Triton extraction method (Con A/Triton membranes) or by filter lysis and purification on sequential sucrose and Renografin® (Squibb Diagnostics, New Brunswick, NJ) gradients (sucrose/Renografin membranes) (35).

ELISA

The titer of R67 IgG before and after adsorption with intact cells or purified plasma membranes was measured in an ELISA (20). Membranes (~0.5 μg/well) in 50 μl of 50 mM sodium carbonate, pH 9.6, were allowed to attach for 14 h at 23°C in 96-well microtiter plates. Blocking, washing, and incubation with a 1:1,000 dilution of horseradish peroxidase-conjugated goat anti-rabbit IgG (Boehringer Mannheim) were performed as described previously (76). Bound antibody was visualized for 5 min with 0.35 mg/ml 2,2′-azino-bis(3-ethylbenzthiazoline-6-sulfonic acid) diammonium salt (Sigma Chem. Co.), 0.02% H_2O_2, 10 mM sodium citrate, pH 4.0, and the absorbance at 410 nm was measured in an MR650 microplate reader (Dynatech, Alexandria, VA).

Immunoblots

Samples were denatured at 70°C for 10 min, run on SDS-polyacrylamide gradient (10–20%) gels (44), electroblotted to nitrocellulose (68), fixed, and blocked (10). For competition experiments, sucrose/Renografin membranes (500 μg) were loaded in a 10-cm well between lanes of prestained molecular mass markers, and the nitrocellulose cut into strips. Ponticulin was visualized with R67 IgG and ^{125}I-labeled protein A (New England Nuclear Dupont), as described (77).

Immunofluorescence Microscopy

All incubations and washes were carried out on ice. Exponentially growing cells at 3–7 × 10^6/ml were harvested, washed three times with Sorensen's buffer, and incubated with either R67 or anti-carbohydrate IgG for 75–90 min with constant shaking (100 rpm). Unbound IgG was removed by washing the cells three times with IgG buffer (17.5 mM potassium phosphate, 0.02% NaN_3, pH 8.0). Primary antibody was visualized by incubating the cells for 45–60 min with rhodamine-conjugated affinity-purified goat anti-rabbit IgG (Cappel, Organon Teknika, Durham, NC). Cells were washed three times with IgG buffer, diluted to ~2 × 10^7/ml, sealed under a coverslip with nail polish, and viewed immediately in a Zeiss (Oberkochen, Germany) MC 100 microscope. Photographic exposures and film development times were held constant at settings optimized for the visualization of ponticulin with R67 IgG in permeabilized cells.

In parallel experiments, cells were fixed and permeabilized with 1% formaldehyde in methanol by the agar overlay method (22), as described previously (77). Cells also were permeabilized with 2% formaldehyde and 0.25% saponin (4). To demonstrate specificity, R67 IgG was mixed with purified ponticulin (0.6 μg/μg IgG) in some experiments.

Results

Isolation of DNA Encoding Ponticulin

A size-selected genomic DNA library was constructed and screened for ponticulin-coding sequences with a nondegenerate 66-bp oligonucleotide (VK11), corresponding to the NH_2-terminal sequence of ponticulin (78). VK11 hybridized to a single 2.9-kb band on Southern blots of genomic DNA cut with EcoRI and HindIII (Fig. 1, *left*). The same 2.9-kb band also was observed on blots probed with a sixfold degenerate 21-mer, containing three inosines, which corresponded to Gly[12] through Val[19] (not shown). This 2.9-kb fragment was isolated and designated pGB (Fig. 2). The insert encoded two open reading frames separated by an AT-rich non-coding region (nt 1327-2509). The second open reading frame constituted the 5′-end of the ponticulin-coding region (nt 2516-2910). Like many *Dictyostelium* genes (27, 40), the 5′-end of the ponticulin gene lacked introns. No canonical splice junctions or intragenic regions with the high A+T content typical of *Dictyostelium* introns were present.

The 3′-sequence of ponticulin was obtained using the technique of PCR-RACE (21). The upstream primer corresponded to nt 14 to 31 of the ponticulin-coding sequence (Fig. 3, *dashed overline*). When the PCR products were analyzed on agarose gels, a single band was observed at ~500 bp. As expected, this band was cleaved by HindIII into two fragments of ~300 and ~200 bp. Seven PCR-RACE clones were isolated and sequenced. Most clones were polyadenylated as shown in Fig. 3; one contained an additional 4 nt before the poly(A) tract. Lengths of the poly(A) tails also varied. All PCR-RACE clones contained the same coding sequence, which exactly matched the overlapping sequence of the genomic clone, suggesting that all clones were derived from one gene, *ponA*. Analyses of genomic Southern blots (Fig. 1, *right*) and a YAC library of *Dictyostelium*

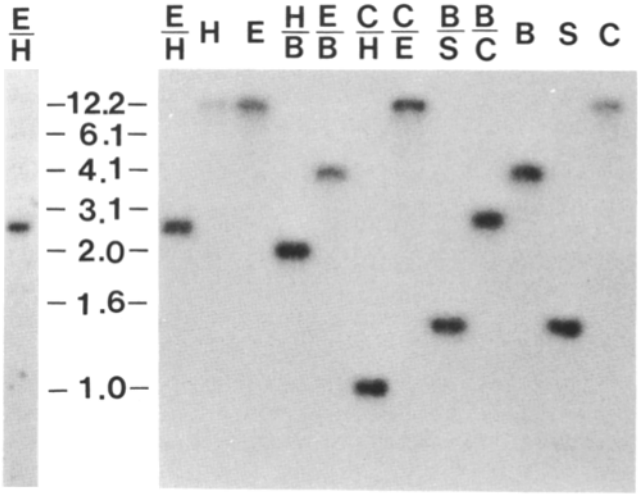

Figure 1. Genomic blots. (*Left*) Genomic DNA probed with the oligonucleotide, VK11. Blot was exposed for 82 h. (*middle*) Sizes of standards in kb. (*right*) Genomic DNA, 10 μg per lane, probed with pT715A (*ponA* sequence; see Fig. 2). Blot was exposed for 44 h. *B*, BglII; *C*, ClaI; *E*, EcoRI; *H*, HindIII; *S*, Sau3A.

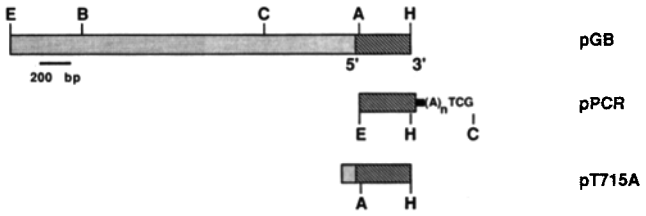

Figure 2. Ponticulin clones and DNA constructs. Structure of the genomic clone (*pGB*), PCR-RACE products (*pPCR*), and exonuclease III fragment (*pT715A*) containing *ponA* sequences. pT715A was generated by exonuclease III digestion of pGB. (*diagonal pattern*) The coding sequence of ponticulin (*ponA*); (*stippling*) flanking sequences. *A*, AflII; *B*, BglII; *C*, ClaI; *E*, EcoRI; *H*, HindIII.

genomic DNA (42); (Kuspa, A., and W. F. Loomis, personal communication) indicate that *ponA* is a single copy gene.

The *ponA* gene encodes a protein of 143 amino acids that has no significant similarity to previously cloned proteins (Fig. 3). The 5'-upstream sequence contains a short G-rich region at nt −238 to −229 (Fig. 3, *underline*) that resembles *Dictyostelium* G-rich enhancer sequences (15). A TATA box (nt −105 to −98) and an oligo(dT) stretch (nt −94 to −78) (Fig. 3, *double underlines*) also are characteristics of transcribed *Dictyostelium* genes (40). Transcription is generally initiated 1-15 bp downstream of such oligo(dT) stretches. A polyadenylation signal (AATAAA) is found at nt 468–473, 36 bp after the TAA stop codon (Fig. 3, *wavy underline*).

The deduced amino acid sequence of the *ponA* gene (Fig. 3) predicts a membrane protein with many properties consistent with those expected for ponticulin. The first methionine is the beginning of a tripartite sequence typical of cleaved eukaryotic signal sequences (70). The positively charged Arg^5 precedes a leucine-rich stretch of 13 hydrophobic amino acids, which is followed by a more polar sequence terminating in Ala^{22}, a preferred residue at signal peptidase cleavage sites. The signal sequence is followed immediately by 23 amino acids (Fig. 3, *heavy underline*) that are identical with the NH_2-terminal sequence determined for plasma membrane-associated ponticulin (78), confirming that cleavage occurs after Ala^{22}. The predicted amino acid composition (Table I) agrees well with that determined for purified ponticulin (11, 78). Both consist of relatively large amounts of serine, threonine, and alanine but little or no methionine or histidine. In agreement with the observed binding of Con A to ponticulin (10, 76), the predicted sequence contains two potential sites for N-linked glycosylation (Fig. 3, *dotted underlines*). The predicted six cysteine residues also are consistent with the observation that disulfide bond(s) stabilize the native, actin-binding conformation of ponticulin (10). Finally, affinity-purified antibodies prepared against bacterial fusion proteins containing the sequence from Gln^{23} through Ser^{130} cross-react with denatured, although not with native, *Dictyostelium* ponticulin (not shown).

The size and developmental expression of the message recognized by *ponA* also are as expected for ponticulin mRNA. Northern blot analysis reveals a single transcript of ~0.8 kb in axenically grown cells (Fig. 4) and in cells grown on bacteria (not shown). This size is close to that expected for the sequence shown in Fig. 3, assuming a poly(A) tail of ~115 bp (53). The amount of this ~0.8-kb mRNA decreases dramatically between 6 and 8 h after onset of starvation-induced development. Such a decrease is consistent with the observation that ponticulin declines in abundance in the plasma membrane between 9 and 12 h of development (35). After 8 h of development, the 0.8-kb message is expressed at a constant, low level (Fig. 4) while the amount of ponticulin in the

```
-265   TTTATTTTTT TAATGATTAC ATTTTTTGTG TGGGGTGTTT CAAAACAATA AAAAGCAATC
-205   CAAAATCCAC AAAAATAAAA AATAAAAATA AAAAAAGGAA GCGAAAAATA AAAAAAAATG
-145   GGTTTATTAT GGTAAAAATG ATTTTAAAAA TTTGAACAGG TATTTAAATT GTTTTTTTTT
 - 85   TTTTTTTTAT TTTTTATTTC CATTCATTAA ATTCAACAAC AAAATCAAAT TCAACAAAAT

 - 25   CAAATCAAAT AATTAATTAA TAAAAATGTT AGTCTTAAGA AATTTATTAG CTTTAGTAAC
                              M  L  V  L  R  N  L  L  A  L  V  T      12

   35   CCTTGCTTTA TTATTCACTT TATCAAGTGC TCAATACACT TTATCCGTTT CAAATTCAGC
         L  A  L  L  F  T  L  S  S  A  Q  Y  T  L  S  V  S  N  S  A    32

   95   CTCAGGTTCA AAATGTACAA CTGCCGTCTC TGCTAAATTA AATGCATGTA ATACTGGTTG
         S  G  S  K  C  T  T  A  V  S  A  K  L  N  A  C  N  T  G  C    52

  155   TTTAAATTCA TTTAATATTG TTGAATCATC AAATGGTAAA GGTTTAGTTT TCAAAACCTT
         L  N  S  F  N  I  V  E  S  S  N  G  K  G  L  V  F  K  T  F    72

  215   TATCAATGCT GCATGTTCTG GTGAATATGA ATCATTATCA CAATTCACTT GTGCTGCTAA
         I  N  A  A  C  S  G  E  Y  E  S  L  S  Q  F  T  C  A  A  N    92

  275   CCAAAAAATC CCAACAACCT CTTACATTGT TTCTTGCAAT TCAACACCAA GCTCAAATTC
         Q  K  I  P  T  T  S  Y  I  V  S  C  N  S  T  P  S  S  N  S   112

  335   AACAACTGAT TCCGATTCCT CAAGTGGTTC AACTGTCATG ATTGGTTTAG CTTCAAGCTT
         T  T  D  S  D  S  S†  S  G  S  T  V  M  I  G  L  A  S  S  L   132

  395   ATTATTTGCT TTTGCCACCT TGTTAGCTTT ATTTTAAatt aatttctata ttctatatat
         L  F  A  F  A  T  L  L  A  L  F  *                           143

  455   agtttaatat ataaataaat aacacccccc tttgtattta atttattaaa aaaaaaaaaa
```

Figure 3. Nucleotide and deduced amino acid sequence of ponticulin. Composite sequence deduced from the 2.9-kb genomic clone encoding ponticulin (nt −265 to +394; residues 1-132) and from PCR-RACE clones (nt 32 to 501; residues 11-143). (*Underlined sequence*) Denotes a G-rich sequence similar to *Dictyostelium* enhancer elements. (*double underlines*) Indicate sequences characteristically found upstream of the transcriptional start sites for transcribed *Dictyostelium* genes. (*dashed overline*) Indicates nucleotides used in the upstream PCR-RACE primer. (*heavy underline*) Indicates the NH_2-terminal sequence of purified ponticulin, as determined by Dr. D. Speicher (Protein Chemistry Facility, Wistar Institute, Philadelphia, PA) (78). The two potential sites for N-linked glycosylation are denoted by dotted underlines, and the predicted site of glycosyl anchor attachment is serine-119 (S^+). The TAA stop codon is indicated with an asterisk, and the consensus sequence for RNA cleavage and polyadenylation (AATAAA) is marked by a wavy underline. These sequence data are available from EMBL under accession number Z36535. Sequence data for the complete genomic clone, including 5'-upstream sequences are available under accession number Z36534.

Table I. Determined and Deduced Amino Acid Compositions of Ponticulin

Amino acid	Purified ponticulin	Deduced aa (Gln^{23}-Ser^{119})	Deduced aa (Gln^{23}-Ser^{143})
	(*mol %*)*	(*mol %*)‡	(*mol %*)§
Asx	10.4 ± 1.1	12.4	9.9
Glx	5.8 ± 0.3	6.2	5.0
Ser	19.8 ± 1.0	21.6	20.7
Gly	9.0 ± 1.9	5.2	5.8
His	0.4 ± 0.8	0.0	0.0
Arg	1.5 ± 1.4	0.0	0.0
Thr	9.3 ± 0.6	11.3	10.7
Ala	10.0 ± 0.8	8.2	9.9
Pro	3.6 ± 0.5	2.1	1.6
Tyr	2.8 ± 0.4	3.1	2.5
Val	5.2 ± 0.4	5.2	5.0
Met	0.7 ± 0.5	0.0	0.8
Cys	4.4 ± 1.1‖	6.2	5.0
Ile	4.4 ± 0.7	4.1	4.1
Leu	6.7 ± 0.7	5.2	9.1
Phe	4.0 ± 0.4	4.1	5.8
Lys	4.0 ± 0.2	5.2	4.1
Trp	ND¶	0.0	0.0

* Average of four determinations with standard deviations, except as noted. Ponticulin was purified by SDS-PAGE and electroblotted onto PVDF before hydrolysis.
‡ Deduced from DNA sequence, assuming glycosyl anchor attachment at Ser-119.
§ Deduced from DNA sequence, assuming no cleavage of the COOH terminus.
‖ Average of two determinations; error indicates measurement range.
¶ Not determined.

plasma membrane decreases slowly (35). Although no increase in the abundance of the 0.8-kb mRNA precedes the increase in the amount of plasma membrane ponticulin observed between 0 and 3 h of development (35), this discrepancy may be attributed to the redistribution of ponticulin from internal stores to the plasma membrane, which apparently occurs during this period (77).

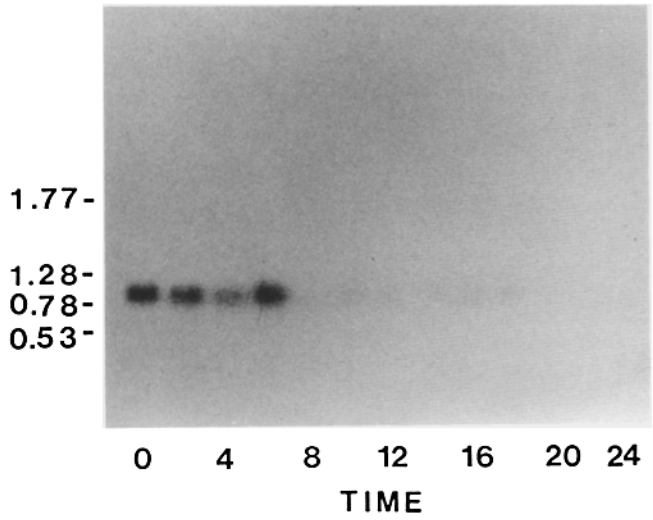

Figure 4. Ponticulin mRNA is downregulated at the onset of cell aggregation and streaming. Northern blot of total RNA (10 μg/lane) isolated from developing *Dictyostelium* at 2-h intervals. The blot was probed with pT715A and exposed to film for 24 h at −80°C. Standards, in kb, are shown on the left.

Predicted Secondary Structure

The structure of ponticulin predicted from the deduced amino acid sequence is very unusual for a transmembrane protein. In addition to the NH_2-terminal hydrophobic α-helical signal sequence discussed above, a second hydrophobic α-helix of 12 residues is predicted at the COOH terminus (Fig. 5, *A* and *B*). Such hydrophobic COOH-terminal α-helices are characteristic of proteins attached to the membrane by glycosyl anchors (19). Furthermore, a cluster of amino acids with small side chains (Ser^{118} to Ser^{122}) is found 10–14 residues before the COOH-terminal hydrophobic domain (Fig. 3). Such a domain is typical of the cleavage/attachment sites for glycosyl anchors. Because glycine or alanine are characteristically found two residues after the glycosyl anchor attachment site (24), Gly^{121} probably corresponds to the ω + 2 position at the recognition site of the COOH-terminal signal transamidase. Thus, the deduced protein sequence strongly suggests that ponticulin contains a glycosyl anchor and that the most probable site of attachment is after Ser^{119}.

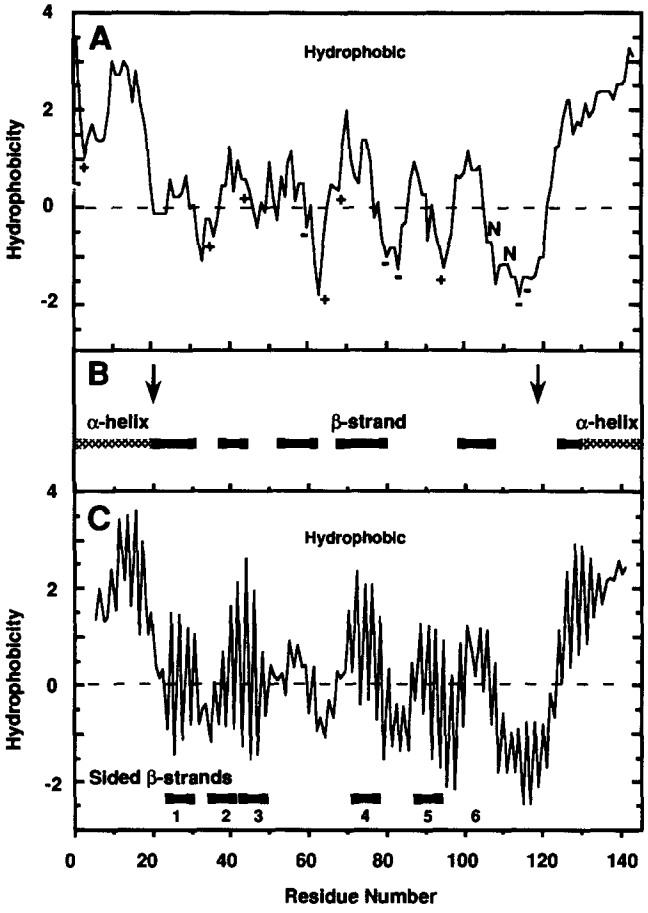

Figure 5. Structural predictions for the deduced sequence of ponticulin. (*A*) Hydrophobicity was calculated according to Kyte and Doolittle (43). *N*, potential N-linked glycosylation sites; +, positively charged residues; −, negatively charged residues. (*B*) Secondary structure predicted by the method of Garnier et al. (23). ↓, predicted polypeptide cleavage sites. (*C*) Sided β-strands (*bars*) identified by the procedure of De Pinto et al. (16). Numbers (*1–6*) denote the potential membrane-spanning β-strands included in the model shown in Fig. 9.

Interestingly, for an integral membrane protein that nucleates actin assembly, no cytoplasmic domain is readily apparent, i.e., no internal stretch of 20–24 α-helical hydrophobic residues (the motif that classically denotes a membrane-spanning domain) is predicted from the *ponA* sequence (Fig. 5, *A* and *B*). However, there are several shorter hydrophobic regions (Fig. 5 *B*), predicted to be β-strands by the Garnier method of analysis (23). These short hydrophobic regions are sufficiently long (8–10 residues) to span the 3-nm-wide hydrophobic core of the *Dictyostelium* plasma membrane (45). Analysis of the periodic distribution of hydrophobicities by the AutoRegressive Moving Average model method (64) also shows that residues 20 through 130 exhibit a power spectral density function that is characteristic of β-sheet structures with an average length of ~11 residues per β-strand (Sun, S., personal communication). Furthermore, several of the short hydrophobic regions are predicted to be amphipathic β-strands with alternating hydrophobic and hydrophilic residues (Fig. 5 *C*) by sided hydropathy analysis (16). A similar analysis (not shown) of porin from *R. capsulatus* correctly predicts nine of the sixteen transmembrane β-strands localized by X-ray crystallography (58, 74), suggesting that this analysis, like most other paradigms for secondary structure predictions (52), is ~56% accurate.

Most of the predicted amphipathic β-strands are flanked by amino acids that are predicted to form β-turns. For instance, both the Garnier paradigm (23) and the turn identification method of Paul and Rosenbusch (54) predict that residues 30–35, 47–52, 62-65, 80-85, and ~96-99 constitute turns that are likely to be exposed to an aqueous environment. Further, the hydrophilic regions between the predicted β-strands tend to be alternately more and less positively charged (Fig. 5 *A*), consistent with alternation across the membrane (71, 79). Thus, although the locations of individual membrane-spanning β-strands are far from certain, four quite different methods for predicting secondary structure agree that the central, membrane-spanning region of the ponticulin sequence demonstrates strong β-strand characteristics. Such unanimity among different prediction schemes increases the likely accuracy of secondary structure predictions to as much as 80% (52).

The actin-binding and nucleating properties of ponticulin strongly support the existence of a cytoplasmic domain which, in turn, requires the presence of transmembrane sequences. In particular, ponticulin's actin nucleation activity is strongly dependent upon the lipid composition of reconstituted vesicles (11), a distinguishing characteristic of integral membrane proteins (32, 38, 55). By contrast, little or no lipid dependence is observed for the activities of proteins that are attached to the membrane solely through a glycosyl anchor, e.g., alkaline phosphatase, 5'-nucleotidase, and acetylcholine esterase (46). An exclusively extracellular localization also is contraindicated by evidence that epitope(s) on ponticulin, which apparently overlap with the binding site for actin, are absent from the surfaces of glutaraldehyde-fixed cells (76). However, the existence of a protein containing both a glycosyl anchor and transmembrane sequences was unprecedented at the time of these experiments. Thus, we looked for the presence of anchor components in ponticulin and critically reexamined the immunological evidence for the presence of a cytoplasmic domain.

Ponticulin Contains A Glycosyl Anchor

In agreement with the prediction from the primary sequence, ponticulin was metabolically labeled with glycosyl anchor components (Fig. 6). Both [^{3}H]palmitic acid (lane *2*) and [^{3}H]ethanolamine (lane *4*), precursor compounds diagnostic for glycosyl anchor addition (19, 46), were biosynthetically incorporated into membrane-bound ponticulin. By contrast, experiments with enzymes that cleave anchor components were inconclusive. Neither phosphatidylinositol-specific phospholipase C (65) nor sphingomyelinase (61) released detectable amounts of ponticulin from purified plasma membranes (not shown). Although consistent with the hypothesis of a membrane-spanning domain, these latter results also would be expected if anchor modifications block cleavage (19, 46).

Comparisons between the determined amino acid composition and that deduced without or with the ponticulin sequence between Ser^{119} and Phe^{143} further support the idea that at least some of the ponticulin isoforms lack this putative cleaved signal sequence (Table I). Relative to the rest of the predicted protein, the COOH-terminal tail is enriched in leucine, phenylalanine, and methionine (Fig. 3). For the first two of these residues, the experimentally determined values (Table I, column *2*) are significantly closer to that expected for ponticulin lacking the COOH-terminal sequence (Table I, column *3*) than they are to the predicted composition of ponticulin containing it (Table I, column *4*). In the case of methionine, experimental variability obscures the difference between 0 and 1 residues. However, the absence of an obvious shift in electrophoretic mobility after treatment with cyanogen bromide (not shown) is consistent with the prior loss of this residue from fully processed ponticulin.

Ponticulin Possesses a Cytoplasmic Domain

R67 IgG, which recognizes native ponticulin, was used to confirm the presence of a cytoplasmic epitope. Using ELISAs (Fig. 7 *A*) and immunoblots (Fig. 7 *B*), we found that isolated plasma membranes, but not equivalent amounts of living cells, adsorbed out essentially all of the titer against ponticulin. This result was independent of the methods used during cell lysis and plasma membrane preparation. Both plasma membranes from Triton-lysed cells (Con A/Triton membranes, Fig. 7, *A* and *B*, lane *3*) and cells lysed mechanically (sucrose/Renografin membranes, Fig. 7 *B*, lane *4*) depleted R67 IgG in these competition experiments. Reactivity also was adsorbed by equivalent amounts of membranes

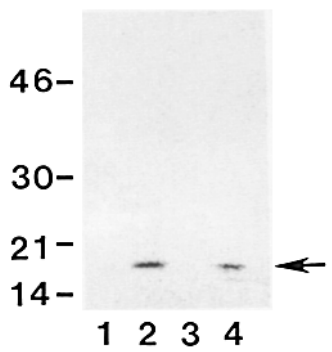

Figure 6. Ponticulin incorporates glycosyl anchor components. [^{3}H]Palmitic acid (lanes *1* and *2*) and [^{3}H]ethanolamine (lanes *3* and *4*) are incorporated into ponticulin (*arrow*). A radiolabeled 17-kD protein is immunoprecipitated with R67 IgG (lanes *2* and *4*), but not with preimmune IgG (lanes *1* and *3*). Molecular masses of standards, in kilodaltons, are shown on the left.

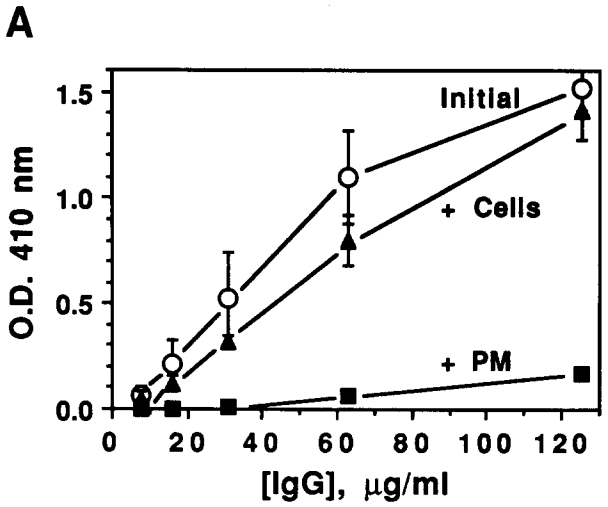

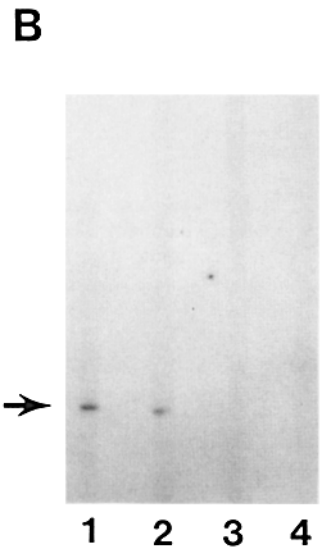

Figure 7. Ponticulin contains an epitope that is exposed in plasma membranes, but not in intact cells. (*A*) Competition experiments. Titer of R67 IgG in an ELISA with Con A/Triton membranes before adsorption (○) and after adsorption with (■) Con A/Triton membranes (0.1 μg/μg IgG) or with (▲) an equivalent amount of intact cells (10^5/μg IgG). Standard errors were calculated from triplicate data points. The experiment was repeated five times with comparable results. (*B*) Immunoblot analysis. Blot strips containing *Dictyostelium* membrane proteins probed with (lane *1*) R67 IgG (10 μg/ml); (lane *2*) R67 IgG adsorbed with living cells (10^5 cells/μg IgG); (lane *3*) R67 IgG adsorbed with Con A/Triton membranes (0.1 μg/μg IgG); (lane *4*) R67 IgG adsorbed with sucrose/Renografin membranes (0.4 μg/μg IgG). The concentrations of cells and membranes represent approximately equal amounts of accessible extracellular membrane surface area. This estimation is based on an average recovery of ~2 mg Con A/Triton membranes per 10^{10} cells (36), representing ~20% of the total surface membrane (35), and on the observation that sucrose/Renografin membranes are sealed vesicles of mixed orientations that are only about half as pure as the unsealed Con A/Triton membrane sheets (26, 35, 48).

from mechanically lysed cells that were purified on sucrose gradients, without exposure to Renografin (not shown).

The epitope(s) recognized by R67 IgG also were exposed by permeabilization of fixed cells. In agreement with previous results (77) R67 IgG recognized both plasma membranes and internal vesicles in cells permeabilized and fixed with cold formaldehyde-methanol (Fig. 8, *A* and *B*). A similar staining pattern was observed in cells permeabilized with 0.25% saponin (not shown). Purified ponticulin blocked the binding of R67 IgG to these sites (Fig. 8, *C* and *D*), confirming the specificity of the antibody in this assay. No binding of R67 IgG to external epitopes on live, unpermeabilized cells was observed (Fig. 8, *E* and *F*). In contrast, a lower titer of an antibody directed mainly against cell surface carbohydrates (76) resulted in bright ring staining of living cells (Fig. 8, *G* and *H*). Taken together, these results indicate the presence of a cytoplasmic domain in ponticulin. The existence of a cytoplasmic actin-binding domain also is supported by the observation that cells containing a disrupted ponticulin gene exhibit little or no high affinity actin-membrane binding in vitro or in vivo (30).

Discussion

In this study, we have determined the primary structure of ponticulin, the only integral membrane protein known to both bind actin and to nucleate actin assembly. The accuracy of the deduced primary sequence (Fig. 3) is supported by protein sequencing (78), comparison with the experimentally determined amino acid composition (Table I), antigenic cross-reactivity between denatured ponticulin and bacterial fusion proteins, and time course of message expression during development (Fig. 4). Extracellular sites in ponticulin are indicated by the apparent processing of both the NH_2- and COOH-termini in the lumen of the endoplasmic reticulum (Figs. 3 and 6), and by the existence of Con A–binding carbohydrates and amino groups accessible to extracellular-labeling reagents (76). Additional extracytoplasmic modification with a glycosyl anchor is indicated by consensus elements in the primary sequence (Fig. 3), metabolic incorporation of anchor precursors (Fig. 5), and comparisons of determined and deduced amino acid compositions (Table I).

Ponticulin also contains a cytoplasmic domain. First, several permeabilizing agents (Triton X-100, mechanical lysis, saponin, methanol/formaldehyde) with quite different mechanisms of action all disclose the ponticulin epitope(s) recognized by R67 IgG (Figs. 7 and 8). Although it may be argued that any one of these permeabilization techniques might result in the exposure of a cryptic extracellular epitope recognized by R67 IgG, it is exceedingly unlikely that all of the treatments would unmask the same epitope. Second, the cytoplasmic protein actin binds directly and with high avidity to ponticulin (10, 76) at a site identical to, or overlapping with, that recognized by R67 IgG (76). Finally, disruption of the ponticulin gene leads to the loss of most of the high affinity binding between actin and the plasma membrane in vivo, as well as in vitro (30). Taken together, these results constitute compelling evidence for the presence of a cytoplasmic domain and indicate that ponticulin must span the plasma membrane, probably via β-strands (Fig. 5). Although the experimental amino acid composition also is consistent with the presence of a certain amount of uncleaved COOH-terminal signal sequence, the immunoprecipitation of [^{3}H]ethanolamine-labeled ponticulin by R67 IgG indicates that at least some of the ponticulin isoforms contain both a glycosyl anchor and the cytoplasmic epitope recognized by R67 IgG.

Structure of Ponticulin

Ponticulin's novel in vitro and in vivo actin-binding and nucleating activities are thus reflected by its unusual struc-

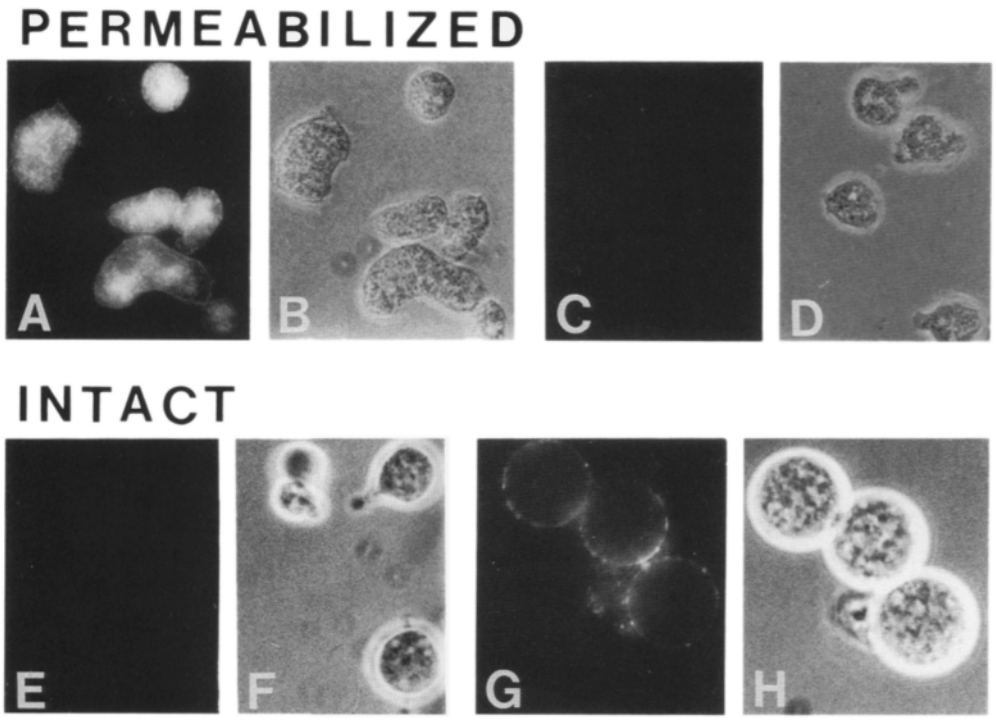

Figure 8. The R67 IgG epitope on ponticulin is exposed in permeabilized, but not intact, cells. *Dictyostelium* amoebae permeabilized with methanol/formaldehyde (*A–D*) and stained with (*A* and *B*) 50 μg/ml R67 IgG or (*C* and *D*) 50 μg/ml R67 IgG in the presence of purified ponticulin (30 μg/ml). Living cells (*E–H*) stained with 100 μg/ml R67 IgG (*E* and *F*) or with 12.6 μg/ml anti-carbohydrate IgG (*G* and *H*). This amount of anti-carbohydrate IgG generates an immunofluorescence intensity approximately equivalent to that observed with 63 μg/ml R67 IgG in permeabilized cells. Even 200 μg/ml R67 IgG produced no detectable fluorescence over background in experiments with intact amoebae. Immunofluorescence (*A*, *C*, *E*, and *G*); phase (*B*, *D*, *F*, and *H*). No staining was observed with secondary antibody alone or with preimmune R67 IgG at the same dilution (not shown).

ture, i.e., the apparent presence of both transmembrane β-strands and a glycosyl anchor (Fig. 9). Given the monomeric behavior of ponticulin (11) and the likelihood that only β-strands organized into a β-barrel can be stably incorporated into the bilayer interior (60), each ponticulin monomer should contain enough β-strands to form a stable β-barrel.

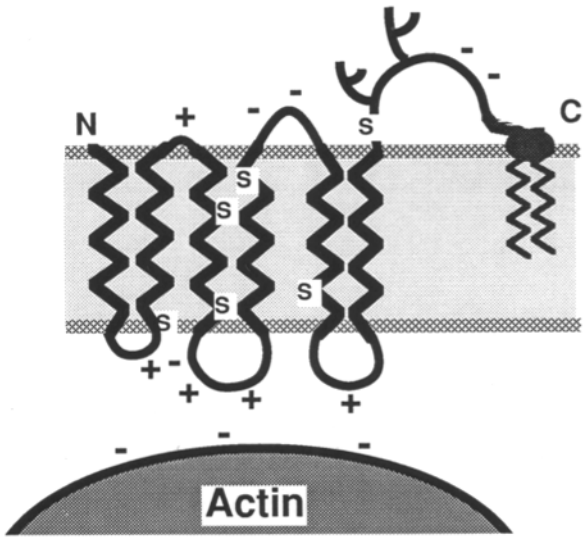

Figure 9. Hypothetical model of ponticulin structure. Because the NH_2- and COOH-termini of ponticulin are both processed in the lumen of the endoplasmic reticulum, transmembrane β-strands must exist in pairs. The six putative membrane-spanning β-strands chosen for this model are numbered at the bottom of Fig. 5 *C*.

Although four β-strands are theoretically sufficient (66), the best-characterized β-barrel proteins contain 8–16 transmembrane β-strands (29, 50, 75), suggesting that the largest reasonable number of β-strands is the most likely. Because both the NH_2- and COOH-termini of the protein are processed in the lumen of the endoplasmic reticulum, membrane-spanning β-strands must occur in pairs. Therefore, we suggest that ponticulin contains either four or six membrane-spanning β-strands, with six being the largest even number of β-strands predicted by structural analyses (Fig. 5).

Although many combinations of four or six membrane-spanning β-strands are conceivable, the six-strand model shown in Fig. 9 agrees well with existing information on protein structure and ponticulin function. First, the model shown in Fig. 9 predicts that the hydrophilic segments of ponticulin are relatively short and close to the membrane bilayer. This prediction is consistent with the observation that native, membrane-bound ponticulin is impervious to digestion by a large number of proteases, including trypsin, chymotrypsin, papain, and proteinase K (Luna, E. J., and A. L. Hitt, unpublished data). This prediction also is consistent with the observation that antibodies to ponticulin are conformationally dependent. Second, the model in Fig. 9 places most of the positively charged lysines in ponticulin on the cytoplasmic surface of the plasma membrane. This localization is consistent with the general "positive-inside" rule of membrane protein structure (71) and with the observation that the interaction between ponticulin and negatively charged actin is predominantly electrostatic (76). Finally, this model places the cysteine residues within the bilayer or at the extracellular surface where they may form the disulfide bond(s) required for the ponticulin-actin interaction (10, 59,

76). Thus, although the model shown in Fig. 9 may err in the details of β-strand number or placement, it is likely that the multipartite binding site(s) on native ponticulin for actin and R67 IgG consist of cytoplasmic loops in a conformation stabilized by disulfide bonds. This structure is completely unlike those of other known actin-binding proteins, which are either soluble proteins or membrane proteins believed to span the membrane via hydrophobic α-helices.

This structure also is unique among those reported for other membrane proteins. Until recently, only ponticulin was thought to contain both a glycosyl anchor and transmembrane peptide domains in vivo. During review of this paper, a surface protein in *S. mansoni* called Sm23 (41) and a protein chimera consisting of the COOH-anchor signal from decay-accelerating factor appended to neutral endopeptidase (33) were both shown to contain glycosylphosphatidylinositol-anchors in addition to cytoplasmic sequences. Unlike ponticulin, however, the transmembrane domains in these proteins are thought to be hydrophobic α-helices. Nevertheless, it is becoming clear that glycosyl anchor addition does not preclude the presence of membrane-spanning sequences.

Previous precedents for multiply attached membrane proteins may have been lacking because glycosyl-anchored proteins are typically identified as such by their release from membranes with anchor-cleaving enzymes. However, this approach cannot possibly detect proteins that also contain transmembrane domains. In fact, multiply attached membrane proteins were proposed as an explanation for the observation that ~10% of the phospholipid-containing membrane proteins in *S. cerevisiae* retain detergent-binding domains after glycosyl anchor removal (13, 67). Also, one explanation for the conformational difference between the normal and abnormal isoforms of the scrapie prion protein is that the abnormal isoform contains two transmembrane α-helices in addition to a glycosyl anchor (62). Such examples suggest that the coexistence of glycosyl anchors and membrane-spanning peptide domains may be more common than currently thought.

Why Anchor a Transmembrane Protein?

Glycosyl anchors appear to have many functions in addition to restricting proteins to the membrane surface. For instance, the glycosyl anchor on ponticulin may be required for proper posttranslational processing. Because it is likely that the putative β-strands must coordinately insert into the membrane (60), the anchor could help promote the assembly of a stable membrane-associated β-barrel. Alternatively, the glycosyl anchor may target ponticulin to particular subdomains of the plasma membrane, control its rate of turnover at the cell surface, and/or mediate interactions with other membrane proteins (2, 5, 9, 39, 63, 80).

In conclusion, this work indicates that ponticulin belongs to a new category of integral membrane proteins, i.e., proteins with both glycosyl anchors and transmembrane peptide domains. In accordance with the numerical nomenclature of Singer (60), we designate this class of membrane proteins as type VI.[2] The availability of the ponticulin gene will facilitate the investigation of the structure, assembly, and functioning of this type VI integral membrane protein.

We thank all the members of the *Dictyostelium* community who generously provided advice, reagents, and encouragement. We are especially grateful to Drs. A. Kuspa and W. F. Loomis for the analysis of their *Dictyostelium* YAC library and to Drs. P. Devreotes, H. Ennis, A. Kaplan, and R. Kessin for providing *Dictyostelium* DNA libraries. We also are grateful to Drs. M. G. Low and S. Udenfriend for gifts of PI-specific PLC and to Dr. Shaojian Sun for performing the ARMA model method of spectral analysis on ponticulin sequences. We thank L. Mattheiss, L. Ohrn, and M. Martineau for excellent technical assistance and Dr. J. Leszyk of the Worcester Foundation W. M. Keck Protein Chemistry Facility for amino acid analyses. We also thank Drs. C. Wilkerson, S. Wadsworth, and R. Jackson for their constructive suggestions throughout the course of this work and Drs. J. Fallon, J. Richter, A. Ross, H. Shpetner, S. Udenfriend, R. Vallee, and Y.-L. Wang for their helpful comments on the manuscript.

This research was supported by National Institutes of Health (NIH) grant GM33048 (E. J. Luna). For portions of this work, A. L. Hitt was supported by NIH grant T32HD07312 to the Worcester Foundation for Experimental Biology. This research also benefited from NIH grant CA54885 to E. J. Luna, the National Cancer Institute Cancer Center Support (Core) grant P30-12708 to the Worcester Foundation for Experimental Biology, and a grant from the J. Aron Charitable Foundation to the Worcester Foundation.

Portions of this work were presented at the 31st, 32nd, and 33rd meetings of the American Society for Cell Biology, Boston, MA, December 8–12, 1991, Denver, CO, November 15–19, 1992, and New Orleans, LA, December 11–15, 1993.

Received for publication 11 April 1994 and in revised form 8 July 1994.

References

1. Altschul, S. F., W. Gish, W. Miller, E. W. Myers, and D. J. Lipman. 1990. Basic local alignment search tool. *J. Mol. Biol.* 215:403–410.
2. Anderson, R. G. W. 1993. Caveolae: where incoming and outgoing messengers meet. *Proc. Natl. Acad. Sci. USA.* 90:10909–10913.
3. Ausubel, F. M., R. Brent, R. E. Kingston, D. D. Moore, J. G. Seidman, J. A. Smith, and K. Struhl. 1989. Current Protocols in Molecular Biology. 1-9.17.3.
4. Baines, I. C., and E. D. Korn. 1990. Localization of myosin IC and myosin II in *Acanthamoeba castellanii* by indirect immunofluorescence and immunogold electron microscopy. *J. Cell Biol.* 111:1895–1904.
5. Barth, A., A. Müller-Taubenberger, P. Taranto, and G. Gerisch. 1994. Replacement of the phospholipid-anchor in the contact site A glycoprotein of *D. discoideum* by a transmembrane region does not impede cell adhesion but reduces residence time on the cell surface. *J. Cell Biol.* 124:205–215.
6. Bennett, V., and D. M. Gilligan. 1993. The spectrin-based membrane skeleton and micron-scale organization of the plasma membrane. *Annu. Rev. Cell Biol.* 9:27–66.
7. Benson, D., D. J. Lipman, and J. Ostell. 1993. GenBank. *Nucleic Acids Res.* 21:2963–2965.
8. Bretscher, A. 1991. Microfilament structure and function in the cortical cytoskeleton. *Annu. Rev. Cell Biol.* 7:337–374.
9. Brown, D. A., and J. K. Rose. 1992. Sorting of GPI-anchored proteins to glycolipid-enriched membrane subdomains during transport to the apical cell surface. *Cell.* 68:533–544.
10. Chia, C. P., A. L. Hitt, and E. J. Luna. 1991. Direct binding of F-actin to ponticulin, an integral plasma membrane glycoprotein. *Cell Motil. Cytoskeleton.* 18:164–179.
11. Chia, C. P., A. Shariff, S. A. Savage, and E. J. Luna. 1993. The integral membrane protein, ponticulin, acts as a monomer in nucleating actin assembly. *J. Cell Biol.* 120:909–922.
12. Cocucci, S. M., and M. Sussman. 1970. RNA in cytoplasmic and nuclear fractions of cellular slime mold amoebas. *J. Cell Biol.* 45:399–407.
13. Conzelmann, A., C. Fankhauser, and C. Desponds. 1990. Myoinositol gets incorporated into numerous membrane glycoproteins of *Saccharomyces cerevisiae*; Incorporation is dependent on phosphomannomutase (SEC53). *EMBO (Eur. Mol. Biol. Organ.) J.* 9:653–661.

2. Type I integral membrane proteins have a single transmembrane stretch with the NH_2 terminus at the cell exterior and the COOH terminus in the cytoplasm; type II proteins also have only a single transmembrane domain, but the orientation is inverted with the NH_2 terminus in the cytoplasm; type III proteins have multiple transmembrane sequences; type IV proteins are aggregates of identical or homologous subunits that, together, constitute a transmembrane channel; and type V proteins are attached to the bilayer only by covalently bound lipids (60).

14. Das, O.-P., and E. J. Henderson. 1983. A novel technique for gentle lysis of eukaryotic cells. Isolation of plasma membranes from *Dictyostelium discoideum*. *Biochim. Biophys. Acta.* 736:45–56.
15. Datta, S., and R. A. Firtel. 1987. Identification of the sequences controlling cyclic AMP regulation and cell-type-specific expression of a prestalk-specific gene in *Dictyostelium discoideum*. *Mol. Cell. Biol.* 7:149–159.
16. De Pinto, V., G. Prezioso, F. Thinnes, T. A. Link, and F. Palmieri. 1991. Peptide-specific antibodies and proteases as probes of the transmembrane topology of the bovine heart mitochondrial porin. *Biochemistry.* 30:10191–10200.
17. den Hartigh, J. C., P. M. P. van Bergen en Henegouwen, A. J. Verkleij, and J. Boonstra. 1992. The EGF receptor is an actin-binding protein. *J. Cell Biol.* 119:349–355.
18. Edidin, M. 1992. Patches, posts and fences: proteins and plasma membrane domains. *Trends Cell Biol.* 2:376–380.
19. Englund, P. T. 1993. The structure and biosynthesis of glycosyl phosphatidylinositol protein anchors. *Annu. Rev. Biochem.* 62:121–138.
20. Engvall, E., and P. Perlmann. 1972. Enzyme-linked immunosorbent assay, ELISA. III. Quantitation of specific antibodies by enzyme-labeled anti-immunoglobulin in antigen-coated tubes. *J. Immunol.* 109:129–135.
21. Frohman, M. A. 1990. RACE: rapid amplification of cDNA ends. *In* PCR Protocols: A Guide to Methods and Applications. M. A. Innis, D. H. Gelfand, J. J. Sninsky and T. J. White, editors. Academic Press, Inc., New York. 28–38.
22. Fukui, Y., S. Yumura, and T. K. Yumura. 1987. Agar-overlay immunofluorescence: high resolution studies of cytoskeletal components and their changes during chemotaxis. *Methods Cell Biol.* 28:347–356.
23. Garnier, J., D. J. Osguthorpe, and B. Robson. 1978. Analysis of the accuracy and implications of simple methods for predicting the secondary structure of globular proteins. *J. Mol. Biol.* 120:97–120.
24. Gerber, L. D., K. Kodukula, and S. Udenfriend. 1992. Phosphatidylinositol glycan (PI-G) anchored membrane proteins. Amino acid requirements adjacent to the site of cleavage and PI-G attachment in the COOH-terminal signal peptide. *J. Biol. Chem.* 267:12168–12173.
25. Goodloe-Holland, C. M., and E. J. Luna. 1984. A membrane cytoskeleton from *Dictyostelium discoideum*. III. Plasma membrane vesicles bind predominantly to the sides of actin filaments. *J. Cell Biol.* 99:71–78.
26. Goodloe-Holland, C. M., and E. J. Luna. 1987. Purification and characterization of *Dictyostelium discoideum* plasma membranes. *Methods Cell Biol.* 28:103–128.
27. Grant, C. E., G. Bain, and A. Tsang. 1990. The molecular basis for alternative splicing of the CABP1 transcripts in *Dictyostelium discoideum*. *Nucleic Acids Res.* 18:5457–5463.
28. Harlow, E., and D. Lane. 1988. Antibodies. A Laboratory Manual. Cold Spring Harbor Laboratory, Cold Spring Harbor, New York. 726 pp.
29. Hill, C. P., J. Yee, M. E. Selsted, and D. Eisenberg. 1991. Crystal structure of defensin HNP-3, an amphiphilic dimer: mechanisms of membrane permeabilization. *Science (Wash. DC).* 251:1481–1485.
30. Hitt, A. L., J. H. Hartwig, and E. J. Luna. 1994. Ponticulin is the major high affinity link between the plasma membrane and the cortical actin network in *Dictyostelium*. *J. Cell Biol.* 126:1433–1444.
31. Hitt, A. L., and E. J. Luna. 1994. Membrane interactions with the actin cytoskeleton. *Curr. Opin. Cell Biol.* 6:120–130.
32. Houslay, M. D., and K. K. Stanley. 1982. Dynamics of Biological Membranes. Influence on Synthesis, Structure and Function. John Wiley & Sons, New York. 330 pp.
33. Howell, S., C. Lanctôt, G. Boileau, and P. Crine. 1994. A cleavable N-terminal signal peptide is not a prerequisite for the biosynthesis of glycosylphosphatidylinositol-anchored proteins. *J. Biol. Chem.* 269:16993–16996.
34. Hynes, R. O., and A. D. Lander. 1992. Contact and adhesion specificities in the associations, migrations, and targeting of cells and axons. *Cell.* 68:303–322.
35. Ingalls, H. M., G. Barcelo, L. J. Wuestehube, and E. J. Luna. 1989. Developmental changes in protein composition and the actin-binding protein ponticulin in *Dictyostelium discoideum* plasma membranes purified by an improved method. *Differentiation.* 41:87–98.
36. Ingalls, H. M., C. M. Goodloe-Holland, and E. J. Luna. 1986. Junctional plasma membrane domains isolated from aggregating *Dictyostelium discoideum* amebae. *Proc. Natl. Acad. Sci. USA.* 83:4779–4783.
37. Jesaitis, A. J., R. W. Erickson, K.-N. Klotz, R. K. Bommakanti, and D. W. Siemsen. 1993. Functional molecular complexes of human N-formyl chemoattractant receptors and actin. *J. Immunol.* 151:5653–5665.
38. Jones, O. T., J. P. Earnest, and M. G. McNamee. 1987. Solubilization and reconstitution of membrane proteins. *In* Biological Membranes. A Practical Approach. J. B. C. Findlay and W. H. Evans, editors. IRL Press Limited, Oxford. 139–177.
39. Keller, G.-A., M. W. Siegel, and I. W. Caras. 1992. Endocytosis of glycophospholipid-anchored and transmembrane forms of CD4 by different endocytic pathways. *EMBO (Eur. Mol. Biol. Organ.)J.* 11:863–874.
40. Kimmel, A., and R. A. Firtel. 1982. The organization and expression of the *Dictyostelium* genome. *In* The Development of *Dictyostelium discoideum*. W. F. Loomis, editor. Academic Press, Inc., New York. 233–324.
41. Köster, B., and M. Strand. 1994. *Schistosoma mansoni*: Sm23 is a transmembrane protein that also contains a glycosylphosphatidylinositol anchor. *Arch. Biochem. Biophys.* 310:108–117.
42. Kuspa, A., D. Maghakian, P. Bergesch, and W. F. Loomis. 1992. Physical mapping of genes of specific chromosomes in *Dictyostelium discoideum*. *Genomics.* 13:49–61.
43. Kyte, J., and R. F. Doolitte. 1982. A simple method for displaying the hydropathic character of a protein. *J. Mol. Biol.* 157:105–132.
44. Laemmli, U. K. 1970. Cleavage of structural proteins during the assembly of the head of bacteriophage T4. *Nature (Lond.).* 227:680–685.
45. Loomis, W. F. 1975. *Dictyostelium discoideum*. A Developmental System. Academic Press, New York. 214 pp.
46. Low, M. G. 1989. The glycosyl-phosphatidylinositol anchor of membrane proteins. *Biochim. Biophys. Acta.* 988:427–454.
47. Luna, E. J., and A. L. Hitt. 1992. Cytoskeleton-plasma membrane interactions. *Science (Wash. DC).* 258:955–964.
48. Luna, E. J., C. M. Goodloe-Holland, and H. M. Ingalls. 1984. A membrane cytoskeleton from *Dictyostelium discoideum*. II. Integral proteins mediate the binding of plasma membranes to F-actin affinity beads. *J. Cell Biol.* 99:58–70.
49. Luna, E. J., L. J. Wuestehube, C. P. Chia, A. Shariff, A. L. Hitt, and H. M. Ingalls. 1990. Ponticulin, a developmentally-regulated plasma membrane glycoprotein, mediates actin binding and nucleation. *Dev. Genet.* 11:354–361.
50. Miller, C. 1991. 1990: Annus mirabilis of potassium channels. *Science (Wash. DC).* 252:1092–1096.
51. Nellen, W., S. Datta, C. Reymond, A. Sivertsen, S. Mann, T. Crowley, and R. A. Firtel. 1987. Molecular biology in *Dictyostelium*: tools and applications. *Methods Cell Biol.* 28:67–100.
52. Nishikawa, K., and T. Noguchi. 1991. Predicting protein secondary structure based on amino acid sequence. *Methods Enzymol.* 202:31–44.
53. Palatnik, C. M., R. V. Storti, and A. Jacobson. 1979. Fractionation and functional analysis of newly synthesized and decaying messenger RNAs from vegetative cells of *Dictyostelium discoideum*. *J. Mol. Biol.* 128:371–395.
54. Paul, C., and J. P. Rosenbusch. 1985. Folding patterns of porin and bacteriorhodopsin. *EMBO (Eur. Mol. Biol. Organ.) J.* 4:1593–1597.
55. Racker, E. 1976. A New Look at Mechanisms in Bioenergetics. Academic Press, New York. 197 pp.
56. Sambrook, J., E. F. Fritsch, and T. Maniatis. 1989. Molecular Cloning. A Laboratory Manual. Cold Spring Harbor Laboratory Press, Cold Spring Harbor, New York. 1–1.47.
57. Sanger, F., S. Nicklen, and A. R. Coulson. 1977. DNA sequencing with chain-terminating inhibitors. *Proc. Natl. Acad. Sci. USA.* 74:5463–5467.
58. Schiltz, E., A. Kreusch, U. Nestel, and G. E. Schulz. 1991. Primary structure of porin from *Rhodobacter capsulatus*. *Eur. J. Biochem.* 199: 587–594.
59. Shariff, A., and E. J. Luna. 1990. *Dictyostelium discoideum* plasma membranes contain an actin-nucleating activity that requires ponticulin, an integral membrane glycoprotein. *J. Cell Biol.* 110:681–692.
60. Singer, S. J. 1990. The structure and insertion of integral proteins in membranes. *Annu. Rev. Cell Biol.* 6:247–296.
61. Stadler, J., T. W. Keenan, G. Bauer, and G. Gerisch. 1989. The contact site A glycoprotein of *Dictyostelium discoideum* carries a phospholipid anchor of a novel type. *EMBO (Eur. Mol. Biol. Organ.) J.* 8:371–377.
62. Stahl, N., D. R. Borchelt, and S. B. Prusiner. 1990. Differential release of cellular and scrapie prion proteins from cellular membranes by phosphatidylinositol-specific phospholipase C. *Biochemistry.* 29:5405–5412.
63. Stefanová, I., V. Horejsí, I. J. Ansotegui, W. Knapp, and H. Stockinger. 1991. GPI-anchored cell-surface molecules complexed to protein tyrosine kinases. *Science (Wash. DC).* 254:1016–1019.
64. Sun, S., and R. Parthasarathy. 1994. Protein sequence and structure relationship ARMA spectral analysis: application to membrane proteins. *Biophys. J.* 66:2092–2106.
65. Taguchi, R., Y. Asahi, and H. Ikezawa. 1980. Purification and properties of phosphatidylinositol-specific phospholipase C of *Bacillus thuringiensis*. *Biochim. Biophys. Acta.* 619:48–57.
66. Tanford, C., and J. A. Reynolds. 1976. Characterization of membrane proteins in detergent solutions. *Biochim. Biophys. Acta.* 457:133–170.
67. Thomas, J. R., R. A. Dwek, and T. W. Rademacher. 1990. Structure, biosynthesis, and function of glycosylphosphatidylinositols. *Biochemistry.* 29:5413–5422.
68. Towbin, H., T. Stahelin, and J. Gordon. 1979. Electrophoretic transfer of proteins from polyacrylamide gels to nitrocellulose sheets: procedure and some applications. *Proc. Natl. Acad. Sci. USA.* 76:4350–4354.
69. Tsukita, S., M. Itoh, A. Nagafuchi, S. Yonemura, and S. Tsukita. 1993. Submembranous junctional plaque proteins include potential tumor suppressor molecules. *J. Cell Biol.* 123:1049–1053.
70. von Heijne, G. 1985. Signal sequences. The limits of variation. *J. Mol. Biol.* 184:99–105.
71. von Heijne, G., and Y. Gavel. 1988. Topogenic signals in integral membrane proteins. *Eur. J. Biochem.* 174:671–678.
72. Wadsworth, S. C., K. Madhavan, and D. Bilodeau-Wentworth. 1985. Maternal inheritance of transcripts from three *Drosophila src*-related

genes. *Nucleic Acids Res.* 13:2153–2170.
73. Warrick, H. M., and J. A. Spudich. 1988. Codon preference in *Dictyostelium discoideum*. *Nucleic Acids Res.* 16:6617–6635.
74. Weiss, M. S., U. Abele, J. Weckesser, W. Welte, E. Schiltz, and G. E. Schulz. 1991. Molecular architecture and electrostatic properties of a bacterial porin. *Science (Wash. DC).* 254:1627–1630.
75. Weiss, M. S., T. Wacker, J. Weckesser, W. Welte, and G. E. Schulz. 1990. The three-dimensional structure of porin from *Rhodobacter capsulatus* at 3 Å resolution. *FEBS (Fed. Eur. Biochem. Soc.) Lett.* 267: 268–272.
76. Wuestehube, L. J., and E. J. Luna. 1987. F-actin binds to the cytoplasmic surface of ponticulin, a 17-kD integral glycoprotein from *Dictyostelium discoideum*. *J. Cell Biol.* 105:1741–1751.
77. Wuestehube, L. J., C. P. Chia, and E. J. Luna. 1989. Immunofluorescence localization of ponticulin in motile cells. *Cell Motil. Cytoskeleton.* 13:245–263.
78. Wuestehube, L. J., D. W. Speicher, A. Shariff, and E. J. Luna. 1991. F-actin affinity chromatography of detergent-solubilized plasma membranes: purification and initial characterization of ponticulin from *Dictyostelium discoideum* plasma membranes. *Methods Enzymol.* 196: 47–65.
79. Yamane, K., and S. Mizushima. 1988. Introduction of basic amino acid residues after the signal peptide inhibits protein translocation across the cytoplasmic membrane of *Escherichia coli*. *J. Biol. Chem.* 263:19690–19696.
80. Yanagishita, M. 1992. Glycosylphosphatidylinositol-anchored and core protein-intercalated heparan sulfate proteoglycans in rat ovarian granulosa cells have distinct secretory, endocytotic, and intracellular degradative pathways. *J. Biol. Chem.* 267:9505–9511.